# Precipitation efficiency and its relationship to physical factors*

Zhou Yu-Shu(周玉淑)[a], Li Xiao-Fan (李小凡)[b]†, and Gao Shou-Ting(高守亭)[a]

[a] *Laboratory of Cloud-Precipitation Physics and Severe Storms (LACS), Institute of Atmospheric Physics, Chinese Academy of Sciences, Beijing* 100029, *China*

[b] *Department of Earth Sciences, Zhejiang University, Hangzhou* 310027, *China*

(Received 30 July 2013; revised manuscript received 14 October 2013; published online 10 April 2014)

The precipitation efficiency and its relationship to physical factors are examined by analyzing a two-dimensional cloud-resolving model simulation during TOGA COARE in this study. The basic physical factors include convective available potential energy, water–vapor convergence, vertical wind shear, cloud ratio, sea surface temperature, air temperature, and precipitable water. Precipitation efficiencies do not show a close relationship to air temperature nor to sea surface temperature nor to precipitable water. The precipitation efficiency increases as the water–vapor convergence rate increases and vertical wind shear weakens, whereas it decreases as the convective available potential energy dissipates and anvil clouds develop.

**Keywords:** precipitation efficiency, water–vapor convergence, convective available potential energy, cloud ratio

**PACS:** 42.68.Ge, 92.60.N–, 92.60.jf, 92.60.Wc **DOI:** 10.1088/1674-1056/23/6/064210

## 1. Introduction

Since Braham (1952) first calculated precipitation efficiency with the inflow of water vapor into a storm through the cloud base as the rainfall source more than half century ago, precipitation efficiency has been used to determine the rainfall intensity in operational precipitation forecasts[1] and various precipitation process studies.[3–7] Early calculations of precipitation efficiency show negative values or beyond a normal range of 0%–100%[8] because the precipitation efficiency is not properly defined, nor are all the rainfall sources included nor are all the rainfall sinks excluded. Sui *et al.*[9] argued that the precipitation efficiency should be defined in precipitation-related budgets that all the precipitation sources can be properly counted and all the precipitation sinks are excluded. Under these definitions, the precipitation efficiency is shown in the normal range of 0%–100%. The precipitation efficiency can be defined in the surface rainfall budget (*LSPE*), cloud microphysical budget (*CMPE*), or rain microphysical budget (*PMPE*).

Gao and Li[10] calculated precipitation efficiency using hourly grid-scale simulation data and found the temporal- and spatial-scale dependence of the precipitation efficiency. They also showed the difference between *LSPE* and *PMPE* and argued that water–vapor process data cannot be used to estimate *PMPE*. *PMPE* deals with the final stage of overall precipitation efficiency, but part of the information in the cloud microphysical budget (*CMPE*) and the surface rainfall budget (*LSPE*) includes how much water vapor actually turns condensed, and of which how much actually forms into precipitation. This means that the precipitation efficiency could be different in different budgets. Recently, Shen *et al.*[11] analyzed a series of equilibrium cloud-resolving modeling data to study the effects of clouds and diurnal variation of sea surface temperature (SST) on precipitation efficiency. They found that the effect of diurnal variation of SST on precipitation efficiency depends on the diurnal magnitude, and the radiative and microphysical effects of ice clouds on precipitation efficiency are opposite. Precipitation efficiency is insensitive to the radiative effect of water clouds. The relationship between precipitation efficiency and basic physical factors such as convective available potential energy, vertical wind shear, water–vapor convergence, and cloud ratio has seldom been studied, while these physical factors have an important influence on the development of rainfall.

In this study, the precipitation efficiencies and their relationships to physical factors will be examined in the surface rainfall budget and the rain and cloud microphysical budgets, respectively, by analyzing a set of two-dimensional (2D) cloud-resolving model simulation data. The model is driven by the large-scale forcing derived from the tropical ocean global atmosphere coupled ocean–atmosphere response experiment (TOGA COARE). In Section 2, the cloud model, forcing, and experiment are described. The results are presented in Section 3. The summary is given in Section 4.

*Project supported by the National Basic Research Program of China (Grant No. 2014CB441402), the National Natural Science Foundation of China (Grant Nos. 41275065, 41075044, and 41075043), and the 985 Program of Zhejiang University.

†Corresponding author. E-mail: xiaofanli@zju.edu.cn

© 2014 Chinese Physical Society and IOP Publishing Ltd 

## 2. Model and experiment

The data analyzed in this study are cited from Li *et al.*[6] The simulation is carried out by using the 2D cloud-resolving model, which was originally developed by Soong and Ogura[12] and Tao and Simpson[13] and was modified by Li *et al.*[14] The model has prognostic equations for mixing ratios of five cloud species and associated cloud microphysical parameterization schemes[15–19] and interactive solar and thermal infrared radiation parameterization schemes.[20–22] The model also has prognostic equations for potential temperature, specific humidity, and perturbation momentums. The basic parameters for the model setup include a horizontal grid mesh of 1.5 km over the model domain of 768 km, 33 vertical levels with a vertical resolution of 40 km near the surface and about 1 km at the top of model, and the time step of 12 s. The experiment is integrated from 0400 LST 18 December 1992 to 1000 LST 9 January 1993 using large scale forcing including vertical velocity, zonal wind, horizontal advections, and sea surface temperature (see Fig. 1 in Ref. [6]). The simulation data are validated with available observational data.[14,23] The simulation data are successfully applied to the analysis of precipitation processes[24] including the surface rainfall process,[25,26] ice microphysics,[27] precipitation efficiency,[6,8–10] and diurnal variation.[28,29] Hourly grid-scale simulation data are used in this study.

## 3. Results

Precipitation sources may be different in different budgets. Precipitation efficiencies can be defined as rain-microphysics (*PMPE*), cloud-microphysics (*CMPE*), and large-scale (*LSPE*), respectively, in rain, cloud and surface rainfall budgets. The rain, cloud, and surface rainfall budgets can be written, respectively, as

$$P_{\rm S} - Q_{\rm RM} = \sum_{I=1}^{12} RP_I, \tag{1}$$

$$P_{\rm S} - Q_{\rm CM} = \sum_{I=1}^{7} P_I, \tag{2}$$

$$P_{\rm S} - Q_{\rm CM} = Q_{\rm WVT} + Q_{\rm WVF} + Q_{\rm WVE}, \tag{3}$$

where

$$P_{\rm S} = \overline{\rho} w_{\rm Tr} q_r|_{z=0}, \tag{4a}$$

$$Q_{\rm RM} = -\frac{\partial [q_r]}{\partial t} - \left[u\frac{\partial q_r}{\partial x}\right] - \left[w\frac{\partial q_r}{\partial z}\right], \tag{4b}$$

$$\begin{aligned} RP_I = {} & ([P_{SACW}(T>T_{\rm o})],[P_{RAUT}],[P_{RACW}],[P_{GACW}(T>T_{\rm o})], \\ & -[P_{REVP}],[P_{RACS}(T>T_{\rm o})], \\ & -[P_{IACR}(T<T_{\rm o})],-[P_{GACR}(T<T_{\rm o})], \\ & -[P_{\rm SACR}(T<T_{\rm o})],-[P_{GFR}(T<T_{\rm o})], \\ & [P_{\rm SMLT}(T>T_{\rm o})],[P_{GMLT}(T>T_{\rm o})]), \end{aligned} \tag{4c}$$

$$Q_{\rm CM} = -\frac{\partial [q_l]}{\partial t} - \left[u\frac{\partial q_l}{\partial x}\right] - \left[w\frac{\partial q_l}{\partial z}\right], \tag{4d}$$

$$\begin{aligned} P_I = {} & ([P_{CND}],[P_{DEP}],[P_{\rm SDEP}],[P_{GDEP}], \\ & -[P_{REVP}],-[P_{MLTG}],-[P_{MLTS}]). \end{aligned} \tag{4e}$$

$$Q_{\rm WVT} = -\frac{\partial [q_v]}{\partial t}, \tag{4f}$$

$$\begin{aligned} Q_{\rm WVF} = {} & -\left[\bar{u}^o\frac{\partial \bar{q}_v^o}{\partial x}\right] - \left[(\bar{w}^o + w')\frac{\partial \bar{q}_v}{\partial z}\right] \\ & -\left[\bar{w}^o\frac{\partial q_v'}{\partial z}\right] - \left[\frac{\partial}{\partial x}(\bar{u}^o + u')q_v'\right], \end{aligned} \tag{4g}$$

$$Q_{\rm WVE} = E_{\rm s}. \tag{4h}$$

Here, $P_{\rm S}$ is the surface rain rate; $\bar{\rho}$ is the air density, which is height–dependent only; $w_{\rm Tr}$ is the terminal velocity for rain ($q_{\rm r}$), which is the mixing ratio of rain; $z$ is the vertical coordinate; $u$ and $w$ are the zonal and vertical components of wind, respectively; $RP_I$ denotes the rainfall source/sink terms from the rain microphysical process; $P_I$ denotes the rainfall source/sink terms from the cloud microphysical process (see Table 1.2 in Ref, [23]); $q_v$ is the specific humidity; $q_l = q_{\rm c} + q_{\rm r} + q_{\rm i} + q_{\rm s} + q_{\rm g}$, where $q_{\rm c}$, $q_{\rm r}$, $q_{\rm i}$, $q_{\rm s}$, and $q_{\rm g}$ are the mixing ratios of cloud water, raindrops, cloud ice, snow, and graupel, respectively; $E_{\rm s}$ is the surface evaporation rate; $T_{\rm o} = 0\,^{\circ}$C. $[(\,)] = \int_{z_{\rm b}}^{z_{\rm t}} \bar{\rho}(\,)\,{\rm d}z$, $z_{\rm t}$ and $z_{\rm b}$ are the heights of the top and bottom of the model atmosphere respectively; $Q_{\rm RM}$ and $Q_{\rm CM}$ are rain and cloud hydrometeor change/convergence, respectively; $Q_{\rm WVT}$ is the local water–vapor change; $Q_{\rm WVF}$ is the water–vapor convergence; Superscript "o" denotes the imposed COARE-observed values; Overbar is a model domain mean, whereas a prime is the perturbation from the model domain mean.

Thus, *PMPE*, *CMPE*, and *LSPE* can be respectively defined as

$$PMPE = \frac{P_{\rm S}}{RSRB}, \tag{5}$$

$$CMPE = \frac{P_{\rm S}}{RSCB}, \tag{6}$$

$$LSPE = \frac{P_{\rm S}}{RSWVCB}, \tag{7}$$

where

$$RSRB = \sum_{I=1}^{12} H(RP_I)RP_I + H(Q_{\rm RM})Q_{\rm RM}, \tag{8a}$$

$$RSCB = \sum_{I=1}^{7} H(P_I)P_I + H(Q_{\rm CM})Q_{\rm CM}, \tag{8b}$$

$$\begin{aligned} RSWVCB = {} & H(Q_{\rm WVT})Q_{\rm WVT} + H(Q_{\rm WVF})Q_{\rm WVF} \\ & + H(Q_{\rm WVE})Q_{\rm WVE} + H(Q_{\rm CM})Q_{\rm CM}. \end{aligned} \tag{8c}$$

Here, *RSRB*, *RSCB*, and *RSWVCB* are the rainfall sources from the rain, cloud, and surface rainfall budgets, respectively; $H$ is the Heaviside function, $H(F) = 1$ when $F > 0$, and $H(F) = 0$ when $F \leq 0$. Expression (8a) shows that the rainfall source in the rain microphysical budget mainly includes the collection of cloud water by rain ($P_{RACW}$) and the melting of graupel ($P_{GMLT}$) and the rain hydrometeor loss/convergence. Expression (8b) reveals that the rainfall source in the cloud microphysical budget mainly contains the vapor condensation and depositions and cloud hydrometeor loss/convergence. Expression (8c) states that the rainfall source in the surface rainfall budget comprises local atmospheric drying, water–vapor convergence, surface evaporation, and cloud hydrometeor loss/convergence. Precipitation efficiencies analyzed in this study are calculated using hourly data and accumulating rainfall sources from each model grid over the model domain.

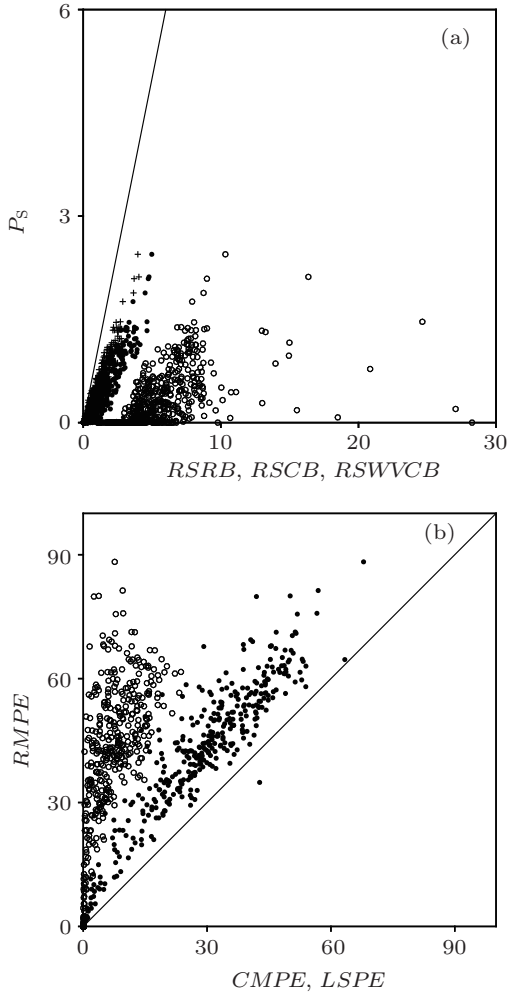



**Fig. 1.** (a) $P_S$ versus *RSRB* (cross), *RSCB* (closed circle), and *RSWVCB* (open circle), and (b) *PMPE* versus *CMPE* (closed circle) and *LSPE* (open circle). Units are mm·h$^{-1}$ for $P_S$, *RSRB*, *RSCB*, and *RSWVCB*, and % for *PMPE*, *CMPE*, and *LSPE*. The straight line in panel (a) denotes $P_S$=*RSRB*, $P_S$=*RSCB*, and $P_S$ = *RSWVCB* whereas the straight line in panel (b) denotes *PMPE* = *CMPE* and *PMPE* = *LSPE*.

*RSRB* is smaller than *RSCB*, whereas these precipitation efficiencies are much smaller than *RSWVCB* (Fig. 1(a)). Thus, *LSPE* is much smaller than *PMPE* and *CMPE*, while *PMPE* is larger than *CMPE* (Fig. 1(b)). Precipitation is much less efficient in the surface rainfall budget than in the rain and cloud microphysical budgets, and is less efficient in the cloud microphysical budget than in the rain microphysical budget. This is due to the fact that large-scale water–vapor processes provide cloud sources through the cloud microphysical budget, and cloud microphysical processes provide rainfall sources via the rain microphysical budget. Thus, large-scale water–vapor sources are stronger than cloud sources, which are stronger than the rainfall sources. Only part of the large-scale water–vapor source is used to generate clouds, and part of the cloud source is used to produce rainfall. The relationship between *PMPE*, *CMPE*, and *LSPE* studied with large-scale forcing in tropical rainfall is consistent with those found in the analysis without large-scale forcing from a series of equilibrium cloud-resolving simulations.[11]

The precipitation is associated with various dynamic and thermodynamic factors. Thus, the relationship between precipitation efficiency and the physical factors will be examined in this study. Mass-weighted mean temperature, sea surface temperature (*SST*) and precipitable water (*PW*) averaged over the model domain denote a vertical mean state of environmental thermal and vapor–water conditions. Convective available potential energy (*CAPE*), calculated for reversible moist adiabatic process[30] over model domain, measures environmental stratification. Model domain mean water–vapor convergence ($Q_{\mathrm{WVF}}$) is associated with upward motions imposed in the model during the model integration. Vertical wind shear affects precipitation through the conversion between model domain mean kinetic energy and perturbation kinetic energy,[31,32] which is calculated by the difference in imposed zonal winds between 10.2 km and 2.7 km in this study. Cloud ratio (*CR*), defined as the ratio of ice–water path (the sum of mass integrations of mixing ratio of cloud ice, snow, and graupel) to liquid water path (the sum of mass integrations of cloud water and rain) by Sui and Li,[33] gauges the relative importance of ice and water clouds. *PMPE* does not show any relationship to the mass-weighted mean temperature, nor to *PW* nor to *SST* (Figs. 2(a)–2(c)). This implies that *PMPE* has a weak relationship to the mean state of environmental conditions. *PMPE* decreases as *CAPE*, $Q_{\mathrm{WVF}}$, and *CR* increase (Figs. 2(d), 2(e), and 2(g)). *PMPE* increases as the negative vertical wind shear weakens (Fig. 2(f)). Since *PMPE* is slightly larger than *CMPE*, and their linear correlation coefficient is 0.92, the relationships between *CMPE* and the physical factors (not shown) are similar to those between *PMPE* and the physical factors (Fig. 2). The student-t test on the significance of the correlation coefficients is further conducted and

the critical correlation coefficient at a 1% significant level is 0.13. Like *PMPE* and *CMPE*, *LSPE* shows relationships with *CAPE*, $Q_{\rm WVF}$, vertical wind shear, and *CR* but does not have any relationship to *SST* (not shown).

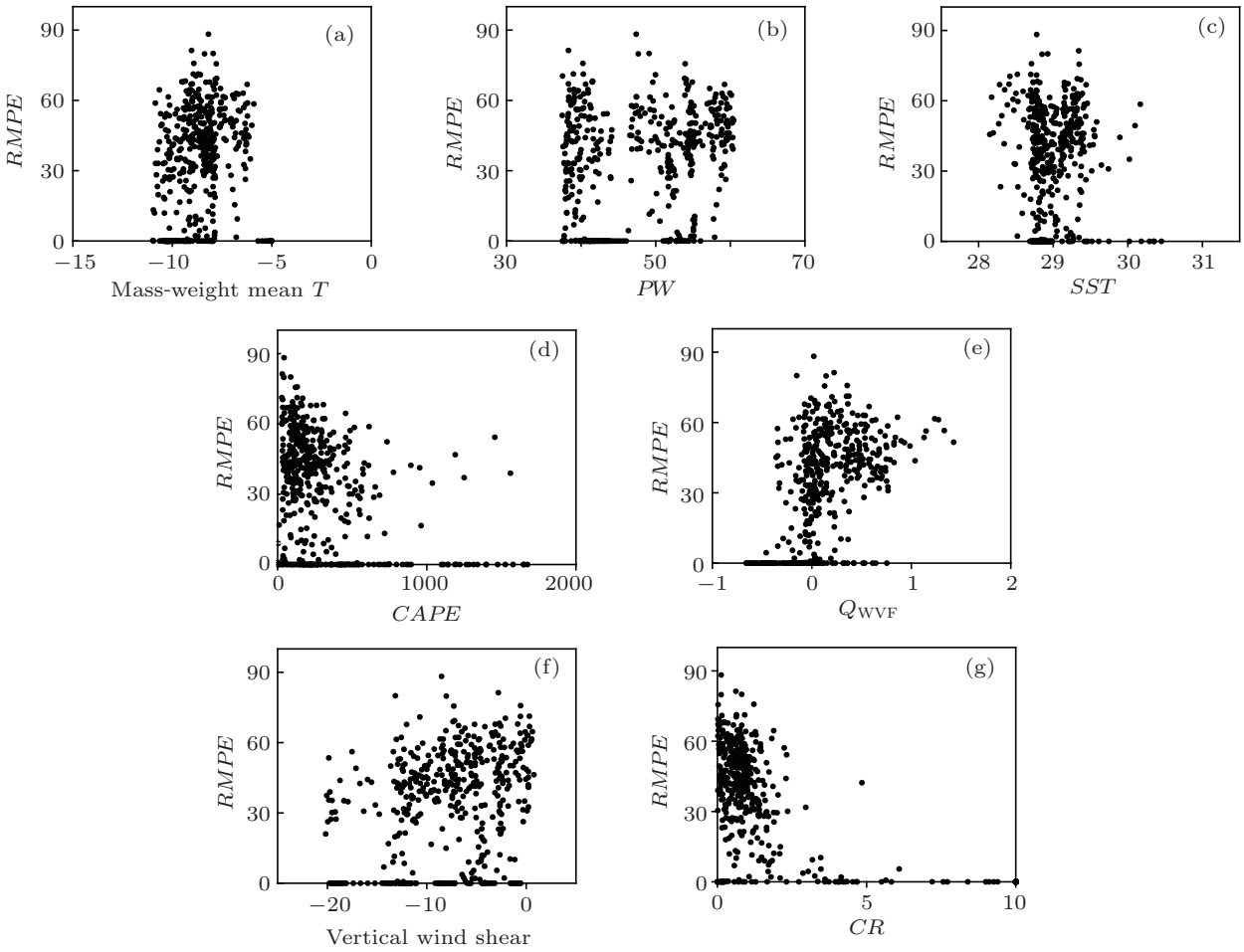



**Fig. 2.** *PMPE* (%) versus (a) mass-weighted mean temperature (°C), (b) precipitable water (*PW*; mm), (c) *SST* (°C), (d) *CAPE* ($\rm J{\cdot}kg^{-1}$), (e) model domain mean water–vapor convergence ($Q_{\rm WVF}$; $\rm mm{\cdot}h^{-1}$), (f) vertical wind shear ($\rm m{\cdot}s^{-1}$), and (g) cloud ratio (*CR*).

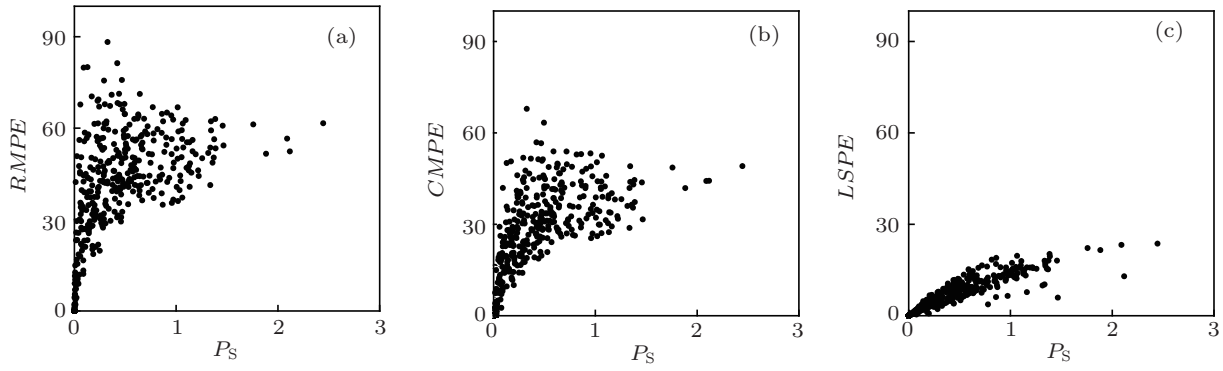



**Fig. 3.** (a) *PMPE* versus $P_{\rm S}$, (b) *CMPE* versus $P_{\rm S}$, and (c) *LSPE* versus $P_{\rm S}$. Units are % for *PMPE*, *CMPE*, and *LSPE*, and $\rm mm{\cdot}h^{-1}$ for $P_{\rm S}$.

To further study the relationship between the precipitation efficiency and the physical factors, we first examine the definition of precipitation efficiency. The definition shows that the precipitation efficiency is proportional to the surface rain rate, which is largely modified by the rainfall source. *PMPE* and *CMPE* have similar magnitudes for surface rain rate and rainfall source (Fig. 1(a)). This implies that the modification from the rainfall source severely scatters the linear relation between *PMPE*/*CMPE* and the surface rain rate, which can be seen in Figs. 3(a) and 3(b). In contrast, the rainfall source (*RSWVCB*)

associated with *LSPE* is much larger than the surface rain rate (Fig. 1(a)), which leads to a linear correlation between *LSPE* and the surface rain rate with a coefficient of 0.92 (Fig. 3(c)). All precipitation efficiencies generally increase as the surface rain rate increases.

Rain rate decreases as *CAPE* increases (Fig. 4(d)) and *CR* increases from 1 to 5 (Fig. 4(g)). The rainfall is a result of the release of *CAPE*. As the rainfall weakens, *CAPE* starts to build up. Such a relationship between rainfall and *CAPE* forms a basic scientific promise that parameterizes cumulus and the associated rainfall for the large-scale circulation model.[34] The increase of *CR* from 1 to 5 favors the development of stratiform clouds. Convective rainfall increases when *CR* increases from 0 to 1. *PMPE* and *CMPE* decrease with *CR* increasing from 0 to 1 (Fig. 2(g)), indicating strong effects of the rainfall source on the modification of the linear relation between precipitation efficiencies and rain rates in rain and cloud microphysical budgets.

The rain rate increases as model domain mean water–vapor convergence increases (Fig. 4(e)) and negative vertical wind shear weakens (Fig. 4(f)). Large-scale vertical velocity is a key force imposed in the cloud model simulation. Thus, the mean water–vapor convergence associated with imposed upward motions is a key process for the production of precipitation as indicated by the similar magnitudes of $Q_{\mathrm{WVF}}$ and $P_{\mathrm{S}}$ in Fig. 4(e). The rainfall source associated with *LSPE* (Fig. 1(a)) is much larger than the mean water–vapor convergence due to a large cancellation between the rainfall source and rainfall sink dominated by water–vapor divergence associated with downward motions in a cyclic later boundary condition furnished in the cloud model used in this study.

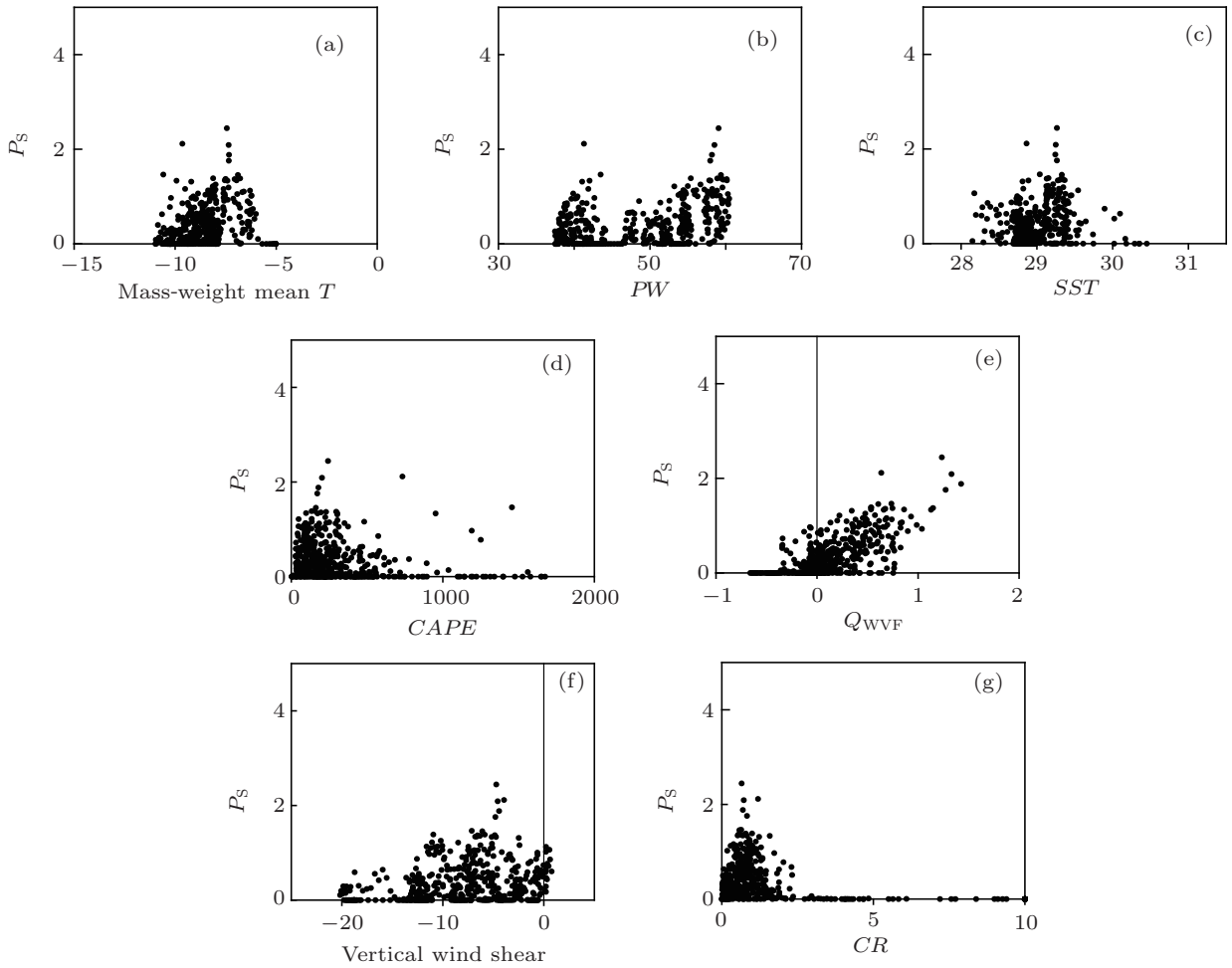



**Fig. 4.** $P_{\mathrm{S}}$ (mm·h$^{-1}$) versus (a) mass-weighted mean temperature (°C), (b) precipitable water (*PW*; mm), (c) *SST* (°C), (d) *CAPE* (J·kg$^{-1}$), (e) model domain mean water–vapor convergence ($Q_{\mathrm{WVF}}$; mm·h$^{-1}$), (f) vertical wind shear (m·s$^{-1}$), and (g) cloud ratio (*CR*).

Rain rate is associated with the secondary circulation, whose intensity is measured by perturbation kinetic energy ($K'$). Thus, the rain rate and perturbation kinetic energy are highly correlated with a coefficient of 0.59 (Fig. 5(a)). Vertical wind shear may affect rainfall by changing the conversion between the model domain mean kinetic energy and the perturbation kinetic energy.[31,32] The conversion between the mean ($\bar{K}$) and perturbation ($K'$) kinetic energy ($C_{\mathrm{u}}(\bar{K},K')$) is a term in the budget of perturbation kinetic energy.[31,32] The tendency of the perturbation kinetic energy ($\partial K'/\partial t$) is negatively correlated with $C_{\mathrm{u}}(\bar{K},K')$ and their linear correlation coefficient is $-0.26$. $C_{\mathrm{u}}(\bar{K},K')$ is positively correlated with the vertical wind shear and

their linear correlation coefficient is 0.14, which marginally exceeds the critical correlation coefficient. Thus, the relationship between rain rate and vertical wind shear cannot be physically explained.

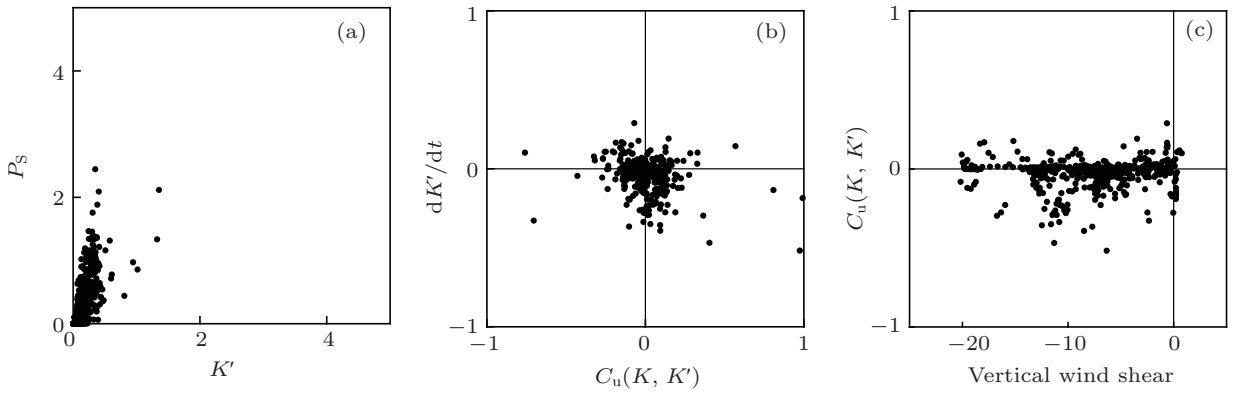



**Fig. 5.** (a) $P_S$ (mm·h$^{-1}$) versus $K'$ ($10^{11}$ J), (b) $\partial K'/\partial t$ ($10^7$ J·s$^{-1}$) versus $C_u(\bar{K},K')$($10^7$ J·s$^{-1}$), and (c) $C_u(\bar{K},K')$ versus vertical wind shear (m·s$^{-1}$).

## 4. Summary

In this study, precipitation efficiency and its association with physical factors are examined. The physical factors include mass-weighted mean temperature, precipitable water, sea surface temperature, convective available potential energy, water–vapor convergence, vertical wind shear, and cloud ratio of the ice–water path to the liquid–water path. The 21-day 2D cloud-resolving model simulation data during TOGA COARE are analyzed in this study. The major results are given below.

(i) Precipitation efficiency defined in a cloud microphysical budget is smaller than that defined in a surface rainfall budget, whereas it is larger than that defined in a rain microphysical budget. Since the rain microphysical budget is a component of the cloud microphysical budget and the cloud microphysical budget is included in the surface rainfall budget, the direct rainfall source is more efficiently consumed to produce precipitation than the indirect rainfall sources.

(ii) The rainfall source from the surface rainfall budget is much larger than those from the cloud and rain microphysical budgets and the surface rain rate. As a result, the precipitation efficiency defined in the surface rainfall budget is much more highly correlated with the rain rate than those defined in the cloud and rain microphysical budgets.

(iii) Precipitation efficiencies increase as the model domain mean water–vapor convergence increases, whereas they decrease as the convective available potential energy increases and ice anvil clouds strengthen. The mean water–vapor convergence is caused by upward motions imposed in the model. The rainfall development is associated with the release of convective available potential energy. The development of the anvil clouds is usually related to the weakening of deep convective precipitation systems during the decay phase.

(iv) Precipitation efficiencies do not have robust relationships to mass-weighted mean temperature nor to sea surface temperature nor to precipitable water nor to vertical wind shear.

## Acknowledgment

The authors thank W. K. Tao for his two-dimensional cloud resolving model, and Prof. M. Zhang, at the State University of New York at Stony Brook, for his TOGA COARE forcing data.

## References

[1] Doswell C A, Brooks H E and Maddox R A 1996 *Wea. Forecasting* **11** 560
[2] Auer A H Jr and Marwitz J D 1968 *J. Appl. Meteor.* **7** 196
[3] Heymsfield G M and Schotz S 1985 *Mon. Wea. Rev.* **113** 1563
[4] Chong M and Hauser D 1989 *Mon. Wea. Rev.* **117** 728
[5] Ferrier B S, Simpson J and Tao W K 1996 *Mon. Wea. Rev.* **124** 2100
[6] Li X, Sui C H and Lau K M 2002 *J. Meteor. Soc. Jpn.* **80** 205
[7] Tao W K, Johnson D, Shie C L and Simpson J 2004 *J. Atmos. Sci.* **61** 2405
[8] Sui C H, Li X, Yang M J and Huang H L 2005 *J. Atmos. Sci.* **62** 4358
[9] Sui C H, Li X and Yang M J 2007 *J. Atmos. Sci.* **64** 4506
[10] Gao S and Li X 2011 *Quart. J. Roy. Meteor. Soc.* **137** 969
[11] Shen X, Qing T and Li X 2013 *Chin. Phys. B* **22** 092413
[12] Soong S T and Ogura Y 1980 *J. Atmos. Sci.* **37** 2035
[13] Tao W K and Simpson J 1993 *Terr. Atmos. Oceanic. Sci.* **4** 35
[14] Li X, Sui C H, Lau K M and Chou M D 1999 *J. Atmos. Sci.* **56** 3028
[15] Lin Y L, Farley R D and Orville H D 1983 *J. Climate Appl. Meteor.* **22** 1065
[16] Rutledge S A and Hobbs P V 1983 *J. Atmos. Sci.* **40** 1185
[17] Rutledge S A and Hobbs P V 1984 *J. Atmos. Sci.* **41** 2949
[18] Tao W K, Simpson J and McCumber M 1989 *Mon. Wea. Rev.* **117** 231
[19] Krueger S K, Fu Q, Liou K N and Chin H N S 1995 *J. Appl. Meteor.* **34** 281
[20] Chou M D, Kratz D P and Ridgway W 1991 *J. Climate* **4** 424
[21] Chou M D, Suarez M J, Ho C H, Yan M M H and Lee K T 1998 *J. Atmos. Sci.* **55** 201
[22] Chou M D and Suarez M J 1994 *NASA Tech. Memo.* **3** 85
[23] Gao S and Li X 2008 *Cloud-Resolving Modeling of Convective Processes* (Berlin: Springer Press)
[24] Li X and Gao S 2011 *Precipitation Modeling and Quantitative Analysis* (Berlin: Springer Press)
[25] Gao S, Cui X, Zhou Y and Li X 2004 *J. Geophys. Res.* **110** D10202
[26] Gao S and Li X 2008 *Quart. J. Roy. Meteor. Soc.* **134** 2127
[27] Gao S, Ran L and Li X 2006 *Mon. Wea. Rev.* **134** 3015
[28] Gao S, Cui X and Li X 2009 *Adv. Atmos. Sci.* **26** 895
[29] Gao S and Li X 2010 *J. Geophys. Res.* **115** D08204
[30] Li X, Sui C H and Lau K M 2002 *J. Atmos. Sci.* **59** 1712
[31] Wang D, Li X, Tao W K and Wang Y 2009 *Atmos. Res.* **94** 270
[32] Shen X, Wang Y and Li X 2011 *Quart. J. Roy. Meteor. Soc.* **137** 236
[33] Sui C H and Li X 2005 *Terr. Atmos. Oceanic Sci.* **16** 419
[34] Arakawa A and Schubert W H 1974 *J. Atmos. Sci.* **31** 674